Robotica (2010) volume 28, pp. 209–214. © Cambridge University Press 2009
doi:10.1017/S0263574709990634

An ultrasound-directed robotic system for microwave ablation of liver cancer

Qiang Huang†, Gui-bin Bian†*, Xing-guang Duan†, Hong-hua Zhao† and Ping Liang‡

† *Intelligent Robotics Institute, Beijing Institute of Technology, 5 Nandajie, Zhongguancun, Haidian, Beijing, China*
‡*Department of Ultrasound, General Hospital of PLA, Beijing, China*

(Received in Final Form: October 27, 2009. First published online: December 7, 2009)

SUMMARY
Hepatocellular carcinoma (HCC), which leads to more than one million deaths every year in the world, is the second most common malignancy in China. As microwave ablation (MWA) is an effective method for the treatment of liver cancer, an ultrasound-directed (US-directed) robotic system was designed to assist surgeons on positioning the needle. This interventional robotic system includes a 5-DOF needle-guiding robot, a conventional 2D ultrasound device, a workstation for path planning and image processing and an electromagnetic tracking device. In clinical environments, we first use real-time freehand 3D ultrasound reconstruction and image analysis methods to attain tumour position, and then manipulate the guiding hole of the robot to position the needle affirmed by the surgeon. Finally, the feasibility of the interventional robotic system are validated by experimental results.

KEYWORDS: Needle insertion; Interventional robot; 3D model reconstruction; Microwave ablation.

1. Introduction

Hepatocellular carcinoma (HCC) is one of the most common malignant neoplasms in the world,[1] which causes more than one million deaths in the world every year.[2] In China, it is the second most common malignancy. Current treatments for HCC mainly include surgical resection and non-surgical treatment. Unfortunately, most patients with primary and secondary liver cancer are not suitable for resection, primarily due to tumour location or underlying liver disease.

Many clinical studies have shown that microwave ablation (MWA) is an effective and safe treatment for liver cancer.[3,4] However, current clinical MWA treatment is manually performed by surgeons. It strongly depends on the surgeon's needling skills against hand tremor, hand–eye coordination and concentration. Only a few experienced surgeons can perform the MWA treatment, which limits it to be used widely in clinics.

For these reasons, it is significant to develop a robotic system to assist a surgeon in executing MWA therapy for patients. Boctor and Taylor proposed the use of two robot arms for ultrasound-directed (US-directed) hepatic ablative therapy which manages both US scanning and needle guiding to overcome the problem of freehand US.[5] However, the system is complicated as it consists of two manipulators, which increases the system's failure rate and is thus inconvenient in clinics.

In this paper, we present an interventional robotic system that assists a surgeon in performing MWA treatment for HCC patients. The robot arm is kept under the guidance of 3D ultrasound (3DUS), which comes from the conventional 2D ultrasound (2DUS) device by a method of 3D freehand reconstruction. This system allows for automatic control of needle hole in a robot arm, along which the surgeon puts the needle into the tumour target. This interventional robotic system can position the liver tumour more accurately and overcome hand tremor, so that the surgeon can concentrate more on planning and monitoring the procedure.

The paper is organized as follows. In Section 2, HCC and its treatments are introduced. The robotic system scheme is given in Section 3. In Section 4, the 3D model reconstruction is provided. In Section 5, three experiments are discussed to validate the system, and conclusion is drawn in Section 6.

2. HCC and Its Treatments

HCC is a liver disease (Fig. 1), which occurs more in Asia, southern Africa and the Pacific Rim area than in other areas. People in every age group have the possibility of suffering from HCC, but more HCC patients can be found in the age group of more than 40 years than in any other age group.

The formation of HCC is a slow process during which genomic changes progressively alter the hepatocellular phenotype to produce cellular intermediates that evolve into HCC.[6] During the long preneoplastic stage, it is hard to be detected and cured. Researches show that HCC's causation is related to hepatitis B virus, hepatitis C virus, long-term use of aflatoxin and heritation.

Currently, there are two major treatments for HCC, surgical treatment and non-surgical treatment.[7]

Surgical treatment is mostly applied in the following cases:

1. When patients are generally in good condition without no obvious heart, lung, kidney disease or other serious organic disease

* Corresponding author. E-mail: bianguibin@bit.edu.cn

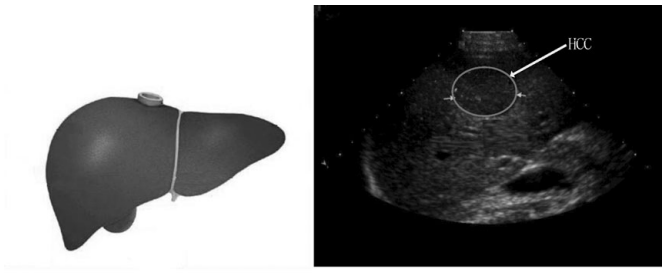

(a) Liver anatomy. (b) The ultrasound image of HCC.

Fig. 1. Liver cancer.

2. When liver functions normally or has only a slight damage (Child-Pugh grade A), or liver function is at grade B, or more serious grade but after a short-term treatment which can return to grade B
3. When the liver functional reserve (such as ICGR 15) is within the normal range
4. When there is no unremovable metastatic liver tumour

However, most liver cancer patients are not suitable for surgical resection because of their poor liver function, the multi centers of tumor and other factors. Therefore, the overall effect of surgical treatment is not ideal.

MWA is a non-surgical treatment for liver tumour. Because it involves a simple operation, inactivating tumour effectively, fewer complications and minor injuries to the patients' bodies, more importance is attached to MWA.

The MWA treatment is mostly applied in the following cases:

1. A single tumour and the tumour is $\leq$5 cm in diameter
2. Multiple tumours; the number of tumours $\leq$3 and the largest tumour $\leq$3–4 cm in diameter
3. No tumour embolus in blood vessels and gall vessels or transfer lesion outside the liver
4. The distance between the liver tumour and the liver's main vessel is at least 5 mm

Currently, clinical MWA treatments are performed manually by surgeons. The general interventional procedure is as follows. First, a CT scan is done over the area around the patient's liver; from the CT image, the surgeon can position the HCC tumour and thereafter suppose a needle path with the liver's surrounding conditions including vessels and other important apparatuses. Then, using the 2DUS image, the surgeon inserts the needle along the pre-planned path to the centre of the liver tumour. However, the interventional performance relies on the surgeon's superior experience and judgement. Furthermore, it also depends strongly on the surgeon's needling skills against hand tremor, hand–eye coordination and concentration; therefore, we developed a US-directed robotic system to assist the surgeon on positioning the needle.

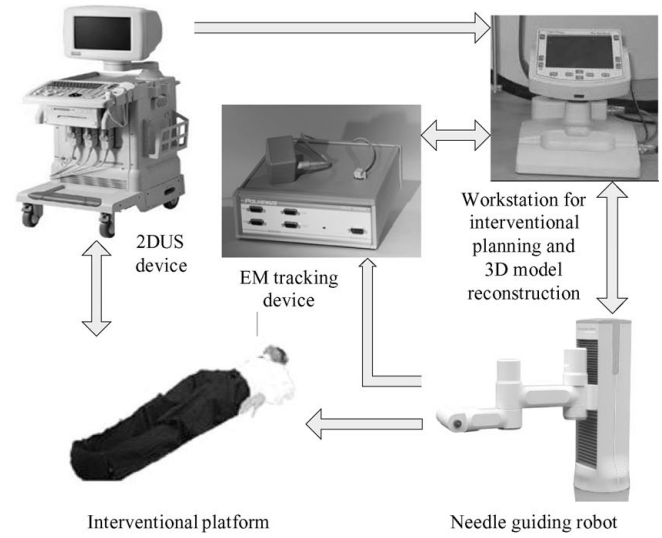

(a) System architecture.

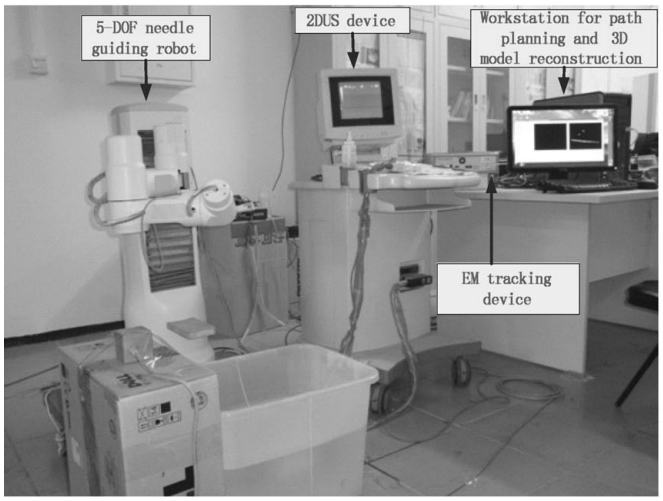

(b) Experiment setup.

Fig. 2. The overall structure of a US-directed robotic system for MWA in liver cancer.

3. A US-directed Robotic System for MWA in Liver Cancer

3.1. System overview

Figure 2 describes the overall structure of a US-directed robotic system for MWA in liver cancer. Major system components include the following:

1. A PC-based interventional workstation providing overall application control, 3D model reconstruction, interventional planning and surgeon interfaces
2. A conventional 2DUS device (WEUT-70X ultrasound machine, China-well, Inc.), which transmits 2DUS images to the workstation via an AV cable.
3. A 5-DOF needle-guiding robot for positioning a needle for MWA
4. An electromagnetic (EM) tracking system (Fastrak, Polhemus, Inc.) connected to the workstation, which is used in 3D model reconstruction with 2DUS images

https://doi.org/10.1017/S0263574709990634 Published online by Cambridge University Press

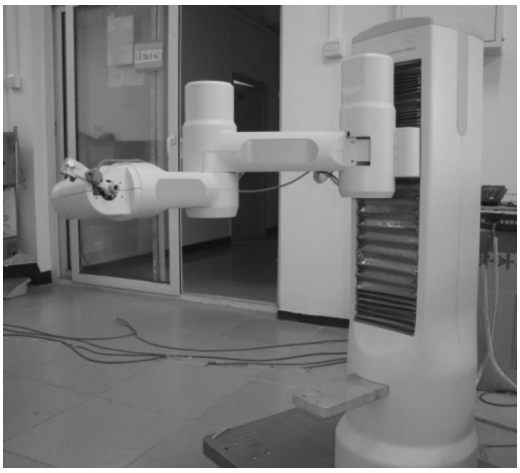

Fig. 3. The prototype of a 5-DOF needle-guiding robot.

3.2. The 5-DOF needle-guiding robot

The needle-guiding robot is used to position the needle-guiding hole. As the revolute along the needle-guiding hole is unnecessary, we designed a 5-DOF needle-guiding robot. The needle-guiding robot consists of a prismatic joint and four revolute joints, as shown in Fig. 3. The first three DOFs are for arm position control, the remaining two DOFs for wrist orientation. The first DOF of the arm moves vertically, and the remaining two DOFs of the arm rotate in the horizontal plane. The first three DOFs determine the position of the guiding-hole in the selected working plane. The last two DOFs are used to control the robot's wrist, which can realise the required orientation of the needle-guiding hole within its workspace.

The obvious advantage of this mechanical structure is its direct motion compared to other configurations of industrial manipulators. The surgeon can understand the motion easily and operate it conveniently, which is important for clinical use. Furthermore, it is also simple to have kinematic analysis; the joints are decoupled in kinematics. When the robot is in motion, the surgeon first manipulates the robot wrist over the patient with the help of four rear joints to reach the desired orientation and then moves the first prismatic joint to the desired position, which can increase the degree of patient safety.

A distributed control system is employed for the robot. All joints use a DC motor. Each joint, which is equipped with an incremental encoder and a hall sensor for getting the absolute position, has a DSP controller. There is an emergency stop in each controller for the DC motor to ensure the system's safety. All DSP controllers communicate with the workstation via RS-422.

3.3. Interventional workstation

The interventional workstation is a 3.0 GHz Pentium 4 computer with 2048 MB of RAM, running on the Windows XP Professional operating system. The workstation is the centre of our experimental setup, and is connected to the ultrasound system, the EM tracking system and both joint controllers. It runs two software suites, one of which is used for robot path planning and the other for US image processing.

The software for robot path planning includes three modules: path planning module, communication module and interventional interface module. The path planning module consists of kinematic analysis and trajectory planning; the communication module deals with the communication between each DSP controller and the interventional workstation; the interventional module deals with the surgeon's selection of trajectory planning.

The software for US image processing mainly includes three modules: 3D reconstruction module, segmentation module and registration module. These three modules will be discussed in detail in the following section.

4. US Image Processing

US image processing mainly has three functions: 3DUS reconstruction, image segmentation and image registration. The detailed process is as follows. In the pre-intervention stage, the zone at and around the tumour zone is scanned with US probe to get 2DUS images together with simultaneous pose data and then the 3D volume is reconstructed with these attained images and semi-automatic segmentation performed on the tumour zone. The surgeon then plans the intervention according to the MWA expert database and determines the pose of the antenna for MWA. In the intervention stage, the featured tissue of liver is scanned to get US images, which are registered to the 3D model that was reconstructed earlier. The surgeon can then monitor the process of MWA treatment for the patient.

4.1. The 3D model reconstruction

A real-time freehand 3DUS reconstruction technique is used to reconstruct the 3D model.[8,9] This technique can dynamically display volume rendering results of the reconstructed volume and sequentially display the reconstructed ratio, which provides both qualitative and quantitative feedbacks on volume reconstruction in real time during acquisition. Therefore, the clinician can know which parts of the tissue have been reconstructed and which parts need further reconstruction in real time during the scanning process, and so the scanning can be done interactively to obtain a relatively integrated 3D image (Fig. 4). Figures 5 and 6 show our experiment results of a plastic phantom.

4.2. Image segmentation

The segmentation of tumour is important in 3D surface reconstruction and display, selection of surgical plane and feature extraction in registration; however, the low quality of US images causes much difficulty in the accurate segmentation of the tumour zone. Furthermore, in the tumour boundary, there are few differences between the tumour and normal tissue; only surgeons can segment the tumour with academic knowledge. So it is unrealistic to realise a totally automatic segmentation, and it is also unrealistic to be involved with much human–computer interaction. We use semi-automatic segmentation to get quick and accurate segmentation of US images. Here we adopted the algorithm of Live-wire segmentation.[10] Our experimental result is shown in Fig. 7.

4.3. Registration

Image registration is a process to determine the mapping relations between two images. There are two criteria for

https://doi.org/10.1017/S0263574709990634 Published online by Cambridge University Press

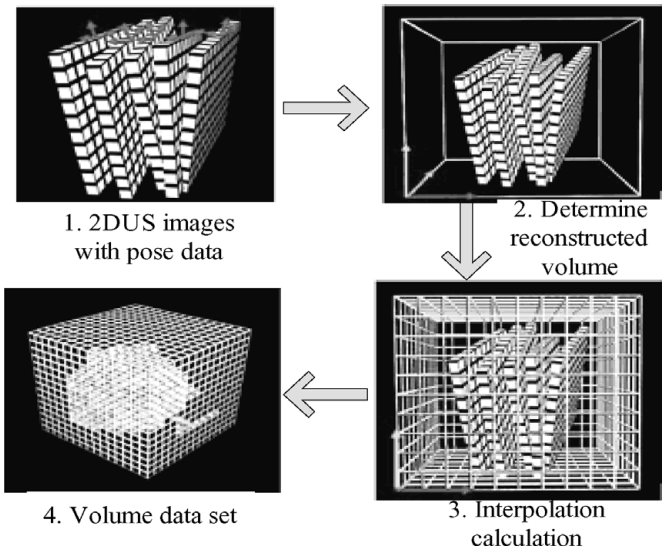

Fig. 4. 3DUS reconstruction framework.

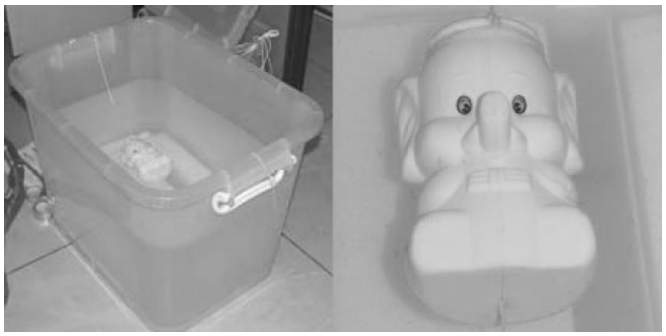

Fig. 5. Phantom for experiment.

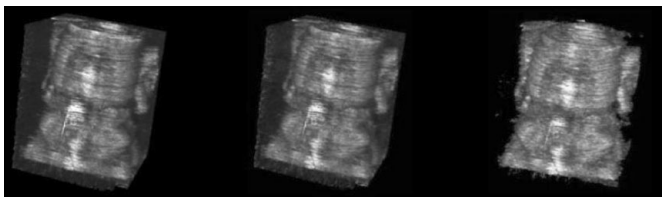

Fig. 6. The result of a 3D model reconstruction.

similarity measurement,[11,12] one is feature-based and the other is voxel-based. The former criterion is to minimise the distance between the corresponding features of the two images, including control point in anatomical structure, 2D boundary line, 3D surface and so on. It is important to extract feature, and then perform feature-based registration. Voxel-based methods use all image information to register images. Because of the poor quality of US images, voxel-based registration has low robustness and has a large failure rate. Thus we adopted the feature-based method to increase the rates of success and safety in intervention.

Feature-based registration can be based on anatomical structures that are easy to locate and have stable and obvious features. In intervention, as the patient's abdomen is inflected by respiration and movement, we adopt feature points such as cross point of vessels to perform registration between 3D pre-intervention images and US images in intervention.

4.4. Coordinate mapping

The target position and orientation in the electromagnetic device coordinate is ${}^{em}T_t$ and the electromagnetic device coordinate in the robot base coordinate is ${}^{r}T_{em}$, and so the target position and orientation in robot base is ${}^{t}T_r = {}^{t}T_{em}\,{}^{em}T_r$ (as shown in Fig. 8).

5. Experiments

We conducted three experiments to evaluate the performance of the robotic system. The first and the second experiments were done separately on a needle-guiding robot and a 3D model reconstruction, the subsystem of the interventional robotic system. The last experiment was done on the whole robotic system to measure the error of the whole system, including the needle-guiding robot and the 3D model reconstruction.

5.1. Accuracy test of the 5-DOF needle-guiding robot

The first experiment was performed as follows. First, we marked a point (as shown in Fig. 9) beside the arm's guiding hole; then we randomly selected a preset point within the

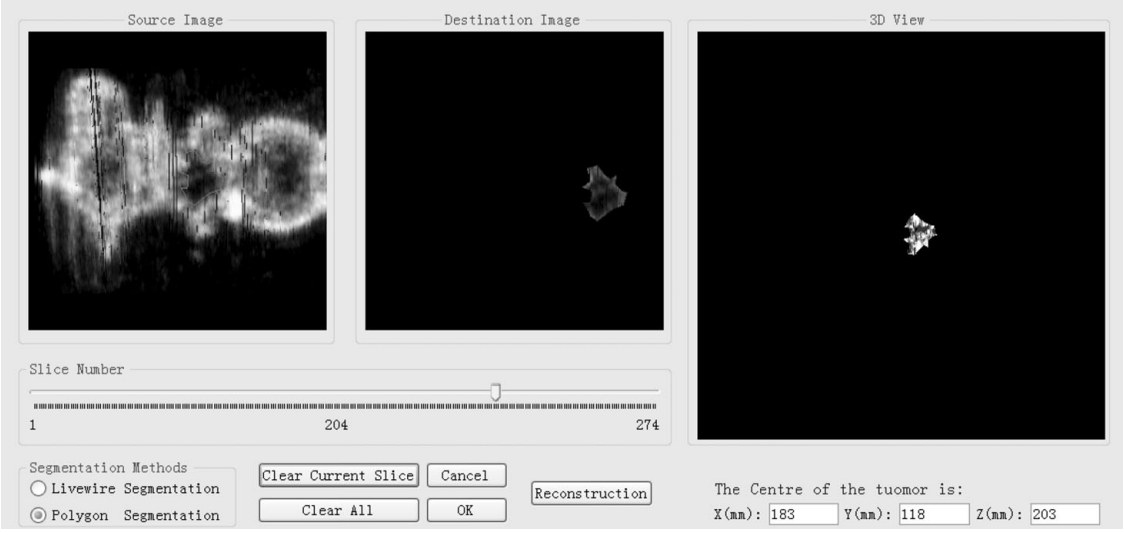

Fig. 7. Experimental result of Liver-wire segmentation.

https://doi.org/10.1017/S0263574709990634 Published online by Cambridge University Press

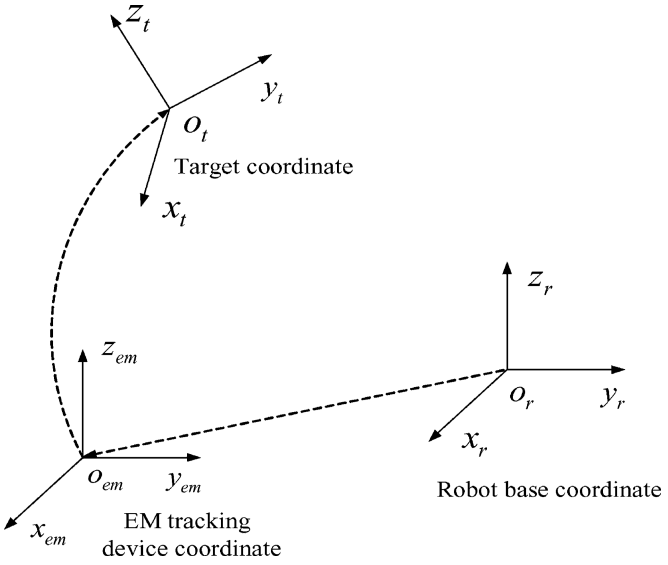

Fig. 8. Coordinate mapping.

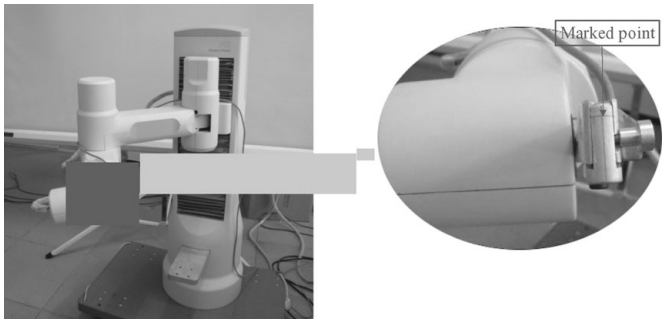

Fig. 9. Accuracy test of a needle-guiding robot.

robot's workspace and solved the joint angles with inverse kinematics; then the robot arm was manipulated to the preset point and the real position of the marked point was measured with a coordinate measure machine after manipulation; finally, the error in Euclidian space was calculated by Eq. (1):

$$\text{err} = \left\| q_{\text{preset}} - q_{\text{arrived}} \right\|. \tag{1}$$

This experiment was repeated 10 times with 10 different preset points. Results show that the maximum error is less than 0.4 mm in Euclidian space. The error mainly comes from the backlash of harmonics and the calibration of the joint angle's zero point.

5.2. Accuracy test of the 3D model reconstruction

The accuracy of the 3D model reconstruction was measured by a needle phantom as shown in Fig. 10. Two stainless steel needles were fixed in a plexiglass to simulate the tumour centre and the puncture point respectively. Three additional landmark points were made in the three aluminium sticks around the needles.

This experiment was done in four steps as follows:

1. The positions of three marked points and two simulation points were measured. The phantom coordinate ${}^{\text{em}}T_{\text{p}}$ was then constructed, and the positions of the simulation points in the phantom coordinate ${}^{\text{p}}q$ were calculated with Eq. (2):

$${}^{\text{em}}q = {}^{\text{em}}T_{\text{p}}^{\text{p}}q. \tag{2}$$

2. The phantom was placed in water and the positions of the three marked points were measured to construct a new transform matrix ${}^{\text{em}}T'_{\text{p}}$, and then the positions of the two simulation points ${}^{\text{em}}q$ were calculated with Eq. (2).
3. The phantom was scanned with a 2DUS machine by selecting the appropriate US plane, and then our US processing software was used to attain the position of the entry point and the target point ${}^{\text{em}}q'$.
4. The error between ${}^{\text{p}}q$ and ${}^{\text{p}}q'$ was calculated with Eq. (3):

$$\text{err} = \frac{\left\| {}^{\text{em}}q'_{\text{entry}} - {}^{\text{em}}q_{\text{entry}} \right\| + \left\| {}^{\text{em}}q'_{\text{target}} + {}^{\text{em}}q_{\text{target}} \right\|}{2}. \tag{3}$$

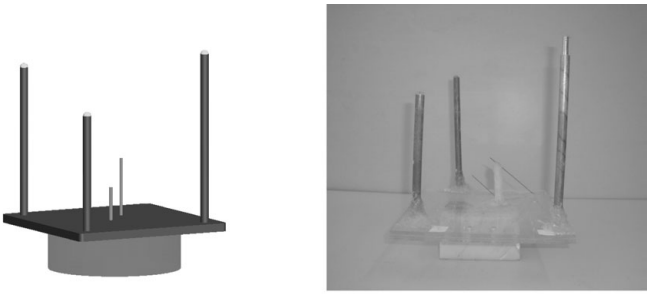

(a) Model of Phantom. (b) Real image of Phantom.

Fig. 10. Phantom for 3D reconstruction experiment.

Fig. 11. Accuracy test of a 3D model reconstruction.

We conducted this experiment 20 times, as shown in Fig. 11, and experiment results show that the accuracy of US-guiding is less than 1.5 mm, which comprises the US calibration error and the EM tracker error.

5.3. Accuracy test of the whole robotic system

The third experiment was done to determine the systemic error of the interventional robotic system on the plastic phantom. A plastic moppet in a tank, as shown in Fig. 9, was introduced to validate the system. We placed five target points on the phantom, and then measured the distance between

https://doi.org/10.1017/S0263574709990634 Published online by Cambridge University Press

the real position of the needle and the preset pin's tip. The procedure for the needle-guiding intervention is as follows:

1. *Exploration and volume scanning*: We use freehand US attached with an EM tracker to search the liver cancer target. After the target is found, we move the US probe to acquire enough 2DUS images with the EM pose information. Then we perform the 3D model reconstruction with these 2D images.
2. *Interventional planning*: After the positions of target point and entry point are attained with the 3D model reconstruction module, the surgeon can plan the trajectory of the robot's needle hole towards the region of ablation with the workstation's display.
3. *Needle-guiding robot motion*: After the interventional planning is affirmed, the surgeon manipulates the needle with the help of the workstation to a certain position, in which the needle hole is over the entry point with a given distance and is parallel with the straight line through the target point and the entry point.
4. *Insertion*: After the needle hole of the robot is ready, the surgeon manually inserts the needle along the needle hole into the target through the entry point. The needle can be inserted with the predetermined depth by the depth marker, and the process is monitored by US probe.
5. *Assessment*: We record the error between the preplanned point and the actual point at which the needle tip reaches.

We have done 30 trials, involving 3 trials for each target point. From the experiment, the average error of 2.5 mm in Euclidean space was acquired. This error comprised the whole interventional robotic system error: the needle guiding and positioning robot's error described earlier and the 3DUS reconstruction including US calibration and EM tracking error. The EM tracking accuracy is about 1.8 mm, as the EM tracking device is disturbed frequently by the magnetic materials or a magnetic device such as a motor, so we manipulate the robot arm far against the tumour target when the tumour zone is scanned to acquire the position of the target point and the entry point. In the intervention case, as the needle insertion is monitored, the surgeon can finely adjust the insertion orientation to get a smaller insertion error.

In future work, we will execute more experiments on phantoms and animals, and other position tracking methods will also be adopted to enhance the performance of the robotic system.

6. Conclusion

In this paper, an efficient US-directed robotic system was presented to execute MWA treatment for liver cancer. First, we synoptically depicted HCC and the application of MWA treatment; then the robotic system solution for MWA was presented, in which the 3D model reconstruction was introduced individually; finally, three experiments were done to measure the performance of the robotic system. The main characteristics of the robotic system are as follows:

1. A 5-DOF needle-guiding robot is developed, whose absolute position error in Euclidian space is less than 0.4 mm.
2. A 3D model reconstruction by freehand US is adopted in the robotic system, with which the surgeon can plan and monitor the intervention more conveniently.
3. Experiment results validate the whole system's feasibility.

There are still some problems to overcome in future work. As the system error of 2.5 mm is a bit larger than expected, some new methods should be adopted to reduce the tracking device error and the US calibration error. Further, *in vivo* animal trials will be conducted before clinical trials can be considered.

Acknowledgements

This work was supported by a High-Tech Research and Development program of China (863 Project) under grant no. 2006AA04Z216 and by the National Natural Science Foundation of China under grant no. 60874048. The authors gratefully acknowledge the support.

References

1. M. Colombo, "Hepatocellular carcinoma," *J. Hepatol.* **15**, 225–236 (1992).
2. C. O. Esquivel, E. B. Keeffe, G. Garcia, J. C. Imperial, M. T. Millan, H. Monge and S. K. So, "Hepatic neoplasms: Advances in treatment," *J. Gastroenterol. and Hepatol.* **14**(Suppl.), 37–41 (1999).
3. T. Seki, M. Wakabayashi, T. Nakagawa, M. Imamura, T. Tamai, A. Nishimura, N. Yamashiki, A. Okamura and K. Inoue, "Percutaneous microwave coagulation therapy for patients with small hepatocellular carcinoma," *Cancer* **85**, 1694–1702 (1999).
4. T. Seki, M. Wakabayashi, T. Nakagawa, T. Itoh, T. Shiro, K. Kunieda, M. Sato, S. Uchiyama and K. Inoue, "Ultrasonically guided percutaneous microwave coagulation therapy for small hepatocellular carcinoma," *Cancer* **74**, 814–825 (1994).
5. E. Boctor, G. Fischer, M. Choti, G. Fichtinger and R. H. Taylor, "A dual-armed robotic system for intraoperative ultrasound guided hepatic ablative therapy: A prospective study," *Proceedings of 2004 IEEE International Conference on Robotics and Automation*, New Orleans, LA (2004) pp. 2517–2522.
6. S. S. Thorgeirsson and J. W. Grisham, "Molecular pathogenesis of human hepatocellular carcinoma," *Nat. Genet.* **31**, 339–346 (2002).
7. Chinese Societies of Liver Cancer and Clinical Oncology, Chinese Anti-Cancer Association; Liver Cancer Study Group, Chinese Society of Hepatology, Chinese Medical Association. "Expert consensus on standardization of the management of primary liver cancer," *tumour*, **29**(3), 295–304 (2009).
8. L. Mercier, T. Langϕ, F. Lindseth and D. L. Collins, "A review of calibration techniques for freehand 3-D ultrasound systems," *Ultrasound Med. Biol.* **31**(2), 143–165 (2005).
9. Y. K. Dai, J. Tian, J. Xue and J. G. Liu, "A qualitative and quantitative interaction technique for freehand 3D ultrasound imaging," *Proceedings of the IEEE EMBS 2006*, New York, (2006) pp. 2750–2753.
10. M. Poona, G. Hamarneh and R. Abugharbieh, "Efficient interactive 3D Livewire segmentation of complex objects with arbitrary topology," *Med. Image Anal.* **32**(8), 639–650 (2008).
11. R. N. Rohling, A. H. Gee and L. Berman, "Automatic registration of 3-D ultrasound images," *Ultrasound Med. Biol.* **24**(6), 841–854 (1998).
12. C. Wachinger, W. Wein and N. Navab, "Registration strategies and similarity measures for three-dimensional ultrasound mosaicing," *Ultrasound Med. Biol.* **15**(11), 1405–1415 (2008).

https://doi.org/10.1017/S0263574709990634 Published online by Cambridge University Press